Th A4 04

High-Order Leapfrog and Rapid Expansion Time Integrations On Staggered Finite Difference Wave Simulations

O.J. Rojas* (BarBarcelona Supercomputing Center / Universidad Central de Venezuela), C. Spa (Universidad Técnica Federico Santa María), J. de la Puente (Barcelona Supercomputing Center)

Summary

This work is an exploratory study of coupling high-order time integrations to a finite-difference (FD) spatial discretization of the 1-D wave equation that combines eigth-order differencing at grid interior, with lateral formulas of order sixth and fourthat boundary neighborhood. This reduction of spatial accuracy at the grid vecinity of free surfaces is a known stability limitation of FD methods, when coupled to the two-step Leap-frog (LF) time stepping, which is widely used on seismic modeling. We first implement LF time integrations with an arbitrary accuracy order, as given from a standard Lax-Wendroff procedure, and compare results from the fourth-, sixth-, and twelfth order schemes, against the popular second-order LF. Our emphirical analyses establish the CFL stability constraints for propagation on an homogeneous medium, as first results, and then consider velocity heterogeneities when assessing dispersion and dissipation anomalies. Finally, we use a rapid expansion method (REM) to approximate the exponential of the semidiscrete FD discretization operator by a truncated Chebyshev matrix expansion. Althougth, REM has been previouslly applied to peudospectral (PS) wave simulations, this REM-FD scheme is the first reported in the technical literature according to our knowledge.

Introduction

This work is an exploratory study of coupling high-order time integrations to a finite-difference (FD) spatial discretization of the 1-D wave equation that combines eigth order $\mathcal{O}(8)$ differencing at grid interior, with lateral formulas of order $\mathcal{O}(6)$ and $\mathcal{O}(4)$ at boundary neighborhood. This reduction of spatial accuracy at the grid vecinity of free surfaces is a known stability limitation of FD methods, when coupled to the two-step Leap-frog (LF) time stepping, which is widely used on seismic modeling. We first implement LF time integrations with an arbitrary accuracy order, as given from a standard Lax-Wendroff procedure, and compare results from the $\mathcal{O}(4)$, $\mathcal{O}(8)$, and $\mathcal{O}(12)$ order schemes, against the popular LF $\mathcal{O}(2)$. Our emphirical analyses establish the CFL stability constraints for propagation on an homogeneous medium, as first results, and then consider velocity heterogeneities when assessing dispersion and dissipation anomalies. Finally, we use a rapid expansion method (REM) to approximate the exponential of the semidiscrete FD discretization operator by a truncated Chebyshev matrix expansion. Althougth, REM has been previouslly applied to peudospectral (PS) wave simulations, this REM-FD scheme is the first reported in the technical literature according to our knowledge.

Theory

We consider the formulation of the 1-D wave equation written in terms of the particle velocity v and stress τ

$$\rho v_t = \tau_x, \quad \tau_t = \mu v_x, \quad \text{for} \quad 0 \leq x \leq 1, 0 \leq t, \tag{1}$$

where $c^2 = \mu/\rho$ is the wave speed, and impose traction free boundary conditions at both end points, i.e., $\tau(0,t) = \tau(1,t) = 0$. A uniform grid of N cells is defined by the nodes $x_i = i \cdot h$, for $0 \leq i \leq N$ and $h = \frac{1}{N}$, where discrete velocities v_i are placed. This grid becomes staggered after including the cell centers $x_{i+1/2} = \frac{x_i + x_{i+1}}{2}$, where unknown stresses $\tau_{i+1/2}$ are located. Numerical differentiation of discrete velocities is performed by using staggered FD stencils that approximate v_x at mid-cell points $x_{i+1/2}$. Likewise, stress differentation is carried out by similar staggered FD stencils that yield τ_x at all grid nodes x_i. This differentation strategy was used by Rojas et al. (2009) on wave propagation problems where mimetic FD stencils have a consistent fourth-order $\mathcal{O}(4)$ accuracy along the whole grid. In this work, we instead adopt standard Taylor-based stencils for staggering FD with accuracy of order $\mathcal{O}(8)$ at most of grid interior points, but gradually reduced to formulas of order $\mathcal{O}(6)$ and $\mathcal{O}(4)$ at the grid vecinity of boundary points. This mixed high-order FD discretization set is better suited when coupling to highly precise time integration strategies. For notation compactness, we collect staggered FD stencils for velocity differentiation in matrix D, while an alterntive matrix G collects the Taylor formulas applied to stresses. Thus, the velocity differentiation process can be simply expressed as $D\mathbf{v}$, being $\mathbf{v} = (v_0, \cdots, v_N)^T$, and similarly, stress derivates can be calculated by $G\tau$, for $\tau = (\tau_{1/2}, \cdots, \tau_{N-1/2})^T$.

Leap-frog (LF) schemes: The formulation of Leap-frog (LF) schemes starts from considering the temporal Taylor expansion of each wavefield, and replacing high-order derivatives for its equivalent spatial derivates through the wave equation (1). The application of this Lax-Wendroff procedure to wave propagation problems is well-known, but most studies limit accuracy to order $\mathcal{O}(4)$, for instance Blanch and Robertsson (1997). In the case of $\mathbf{v}$, this procedure leads to the LF scheme of order $\mathcal{O}(k+1)$, for $k = 1, 3, 5, \ldots$, and given by

$$\mathbf{v}^{n+\frac{1}{2}} = \mathbf{v}^{n-\frac{1}{2}} + pG\tau^n + \frac{1}{24}p^3(GD)G\tau^n + \frac{1}{1920}p^5(GD)^2G\tau^n + \cdots + \frac{1}{2^{k-1}k!}p^k(GD)^{\frac{k-1}{2}}G\tau^n. \tag{2}$$

Above, p corresponds to the CFL stability parameter $p = \frac{c\Delta t}{h}$, and Δt is the time step. For the system (1), LF schemes take advantage of the time staggering of velocities with respect to stresses, which is denoted by the supra indexes on discrete variables. A similar expansion represents the LF calculation of τ^{n+1}, where τ^n and $(GD)^{\frac{k-1}{2}}G$ terms are replaced by $\mathbf{v}^{n+\frac{1}{2}}$ and $(DG)^{\frac{k-1}{2}}D$, respectively. At the implementation level, a new high-order term in (2) is computed by two succesive spatial differentiations of the previous term, using matrices D and G, and storing temporary results on two auxiliary memory vectors.

At this point, we undertake a comparative stability analysis among LF integration methods. The goal is finding the maximum CFL p^{MAX} that avoids exponentially growing instabilities as $n \to \infty$ for fixed

Δt. Here, this p value results from a matrix analysis that requires every method be written as a one-step iteration $\phi^{n+1} = T(p)\phi^n$. The threshold p^{MAX} corresponds to the maximum CFL, at which the spectral radius of T stays bounded by 1. Thus, we define $\phi^{n+1} = (\mathbf{v}^{n+\frac{1}{2}}, \tau^{n+1})$ and find the expression of $T(p)$ according to (2), and to the similar expansion for stress updating. In this work, we restrict this study to the LF schemes with accuracy $\mathcal{O}(2)$, $\mathcal{O}(4)$, $\mathcal{O}(8)$, and $\mathcal{O}(12)$ order, and corresponding p^{MAX} values are listed in Table 1.

LF scheme	$\mathcal{O}2$ (LF2)	$\mathcal{O}4$ (LF4)	$\mathcal{O}8$ (LF8)	$\mathcal{O}12$ (LF12)
p^{MAX}	0.815	2.324	2.816	2.840

Table 1: Maximum CFL p values for time integration Leap-frog schemes

A rapid expansion method (REM): The formulation starts after writing the model (1) in the following semidiscrete form, where time dependences remain continuous,

$$\dot{\phi}(t) = A_h\phi(t), \quad \text{where} \quad A_h = \frac{c}{h}\begin{bmatrix} 0_{N+1} & G \\ D & 0_N \end{bmatrix} \quad \text{and} \quad \phi(t) = (\mathbf{v}(t), \tau(t)). \tag{3}$$

Above, 0_{N+1} and 0_N represent zero matrices with sub-indexed dimensions. The exponential matrix operator allows time updating the discrete solutions by the iterative formula $\phi(t^n + \Delta t) = expm(\Delta t A_h)\phi(t^n)$. The accuracy and computing cost of this REM scheme strongly depends on the approximation of $expm$, and Tal-ezer et al. (1987) employs the truncated expansion of Chebyshev matrix polynomials

$$expm(\Delta t A_h) \sim \sum_{k=1}^{M} C_k J_k(R\Delta t) Q_k\left(R^{-1}A_h\right) \quad \text{where} \quad R = \frac{c}{h} max\{eig(A)\}. \tag{4}$$

Above, $A = (h/c)A_h$, J_k represents the kth Bessel function of first kind, $C_0 = 1$, and $C_k = 2$ for $k \geq 2$. The Chebyshev polynomials Q_k satisfy the well-known three-term recurrence relation $Q_{k+1}(w) = 2wQ_k(w) + Q_{k-1}$, $k \geq 0$, with initial iterates $Q_0(w) = I$ and $Q_1(w) = w$, for w a matrix argument. The scaling parameter R can be estimated from a bound for the eigenvalue spectrum of dimensionless matrix A. In our FD implementation, we use the Gershgorin spectrum estimation given by the sum of the absolute coefficients of the first lateral G stencil, i.e., $max\{eig(A)\} \leq |g_{11}| + |g_{12}| + \cdots$.

The total number M of non-neglected terms is a crucial implementation parameter, and Pestana and Stoffa (2010) relates M with the parameter $R\Delta t$, for a convenient R estimation in the case of PS methods. In this work, we find that M also results critical for stability purposes, and the higher is set up the CFL p parameter, the more terms must be computed. For a representative set of p values, table 2 lists the minimum number of Chebyshev terms M^{MIN}, above which the spectral radius of $expm(\Delta t A_h)$ (approximated by (4)) is ~ 1, within a tolerance of 10^{-12}. For $M \geq M^{MIN}$, this REM implementation behaves stably and more accurate than LF schemes in our numerical experimentations, as described in next section. Here, we only compute REM solutions for parameters $p = 2$ and $M = 32$, which are used as highly accurate references for LF solutions.

CFL p	0.5	1	2	10	50
M^{MIN}	18	25	34	105	390

Table 2: Minimum number of terms in REM series (4) for stable time integrations

Numerical example

In our numerical tests, wave motion takes place on a 1-D acoustic medium with one optional velocity discontinuity, and both ends acting as free surfaces. The interior heterogeneity contrast depends on a scalar $\alpha \geq 1$, such that acoustic speed might jump from c to αc, for waves crossing this point from left to right. The initial stress distribution comprises two Ricker wavelets, and each pulse is centered on one of the two homogeneous material blocks. Both wavelets have same strain energy content with opposite amplitude signs for destructive interference at the junction point. The domain length and global

simulation time are chosen in such a way that, periodically, the stress distribution becomes identical to the initial condition, so we can quantify numerical errors in terms of envelope and phase misfits (EM and PM). Hovewer, we only calculate EM and PM on the left material block with lower acoustic speed in case that $\alpha > 1$, given that shorter wavelengths would be observed on this block for a reference frequency, and therefore have a coarser sampling on our uniform gridding simulations. When computing our numerical solutions, we explore a set of spatial resolutions (4, 6, 8, 10, 12 and 14 poins per minimum wavelength, *ppw*) and propagation distances are measured in terms of the dominant wavelength λ^{DOM}. The setting of *ppw* and λ^{DOM} is done according to the initial Ricker wavelet on the left segment with a possibly smaller breadth. Because of the CFL stability limit and computational costs increase with the time discretization order, we adjust time steps in all simulations according to CFL = 0.5 (in the case of LF2), CFL = 1.6 (in the cases of LF4, LF8 and LF12), and CFL = 2 (in the case of REM). Under these conditions, and taking the computing cost of one LF2 iteration as reference, the CPU cost per iteration of alternative schemes is $\sim$ 1x, 3x, 5x, and 8x, in case of LF4, LF8, LF12, and REM (adding $M = 34$ terms in (4)), respectively.

Results

For each numerical scheme, figures 1,2, and 3 display the relative EM and PM misfits obtained in simulations for three different wave speed configurations, namely α = 1, 2, and 5, respectively. Each scheme is identified by a particular symbol, while different line styles represent the amount of wavelengths λ^{DOM} traveled by the reference Ricker pulse on the left acoustic block. Here, we only show misfits for three representative traveling distances of $40\lambda^{DOM}$ (solid lines), $80\lambda^{DOM}$ (dashed lines), and $120\lambda^{DOM}$ (dotted lines). For an homogeneous medium, both EM and PM misfits respond well to the order of time discretization, and for any given combination of grid sampling and propagation distance, LF2 solutions are the least accurate, while accuracy of REM solutions is not reached by any LF scheme. The significant similarity of LF8 and LF12 errors is remarkable, and show that LF corrections of high-order Taylor terms are lost probably due to the arithmetic limitation. For a typical resolution assessment, let us consider LF4 misfits on grids with 6 *ppw*, and notice that the LF2 method would require grids with 14 *ppw* to yield nearly similar EM and PM errors. Same conclusion holds when taking LF8-LF12 (or REM) misfits at 6 *ppw* with respect to LF4 (or LF8-LF12) errors at 14 *ppw*. In the case of heterogenous media, discrepancies on the accuracy of high-order LF methods reduce for α = 2, and finally leads to indistinshable LF4-LF8-LF12 errors when α = 5. On these tests with α = 5, notice that LF2 and REM continue to be the least and the most accurate schemes, respectively, but on grids with resolution of 8 *ppw* and higher.

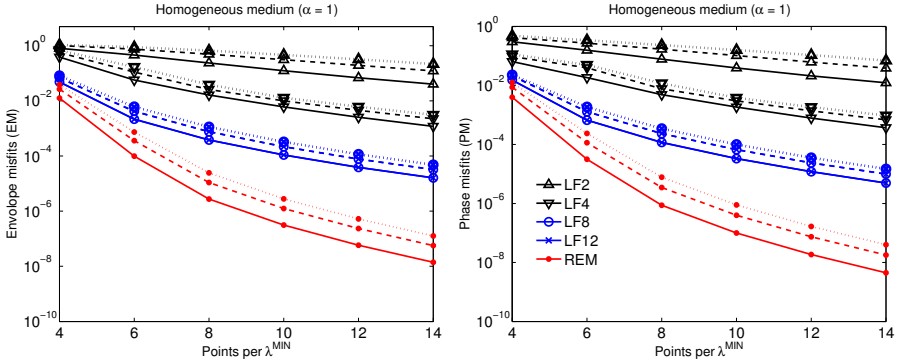

Figure 1: EM and PM errors of LF and REM simulations on a homogeneous medium ($\alpha = 1$).

An alternative comparison is based on establishing our accuracy tolerance on 1% (EM = PM = 0.01), and identifying the minimum grid sampling required to satisfy such tolerance at a propagation distance of $40\lambda^{DOM}$, for instance. To do so, let us retake simulations on the homogeneous medium. Coarsely speaking, the LF8, LF12 and REM methods achieve this accuracy target on the EM metric on grids with 4 *ppw*, while LF4 requires grids twice denser (i.e., a sampling of 8 *ppw*), and the LF2 scheme needs meshes with at least 14 *ppw*. For each of these methods, a similar meshing is enough to satisfy the same tolerance on PM errors, given than phases are better modeled than amplitudes, for any combination of propagation distance and grid resolution. When heterogeneities are considered EM and PM misfits

globally decay, so similar lower sampling advantanges of LF8, LF12, and REM methods with respect to LF4 and LF2 schemes, can be observed for smaller error tolerances, for instance 0.01% (EM = PM = 0.0001) in the case of $\alpha = 5$.

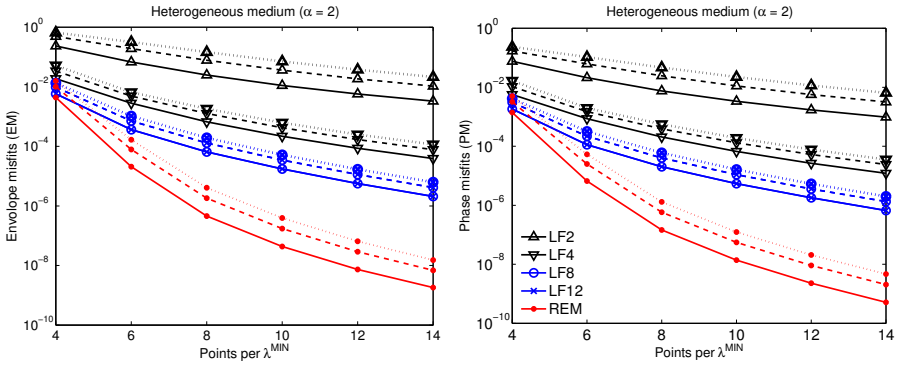

Figure 2: EM and PM errors of LF and REM simulations on a heterogeneous medium ($\alpha = 2$).

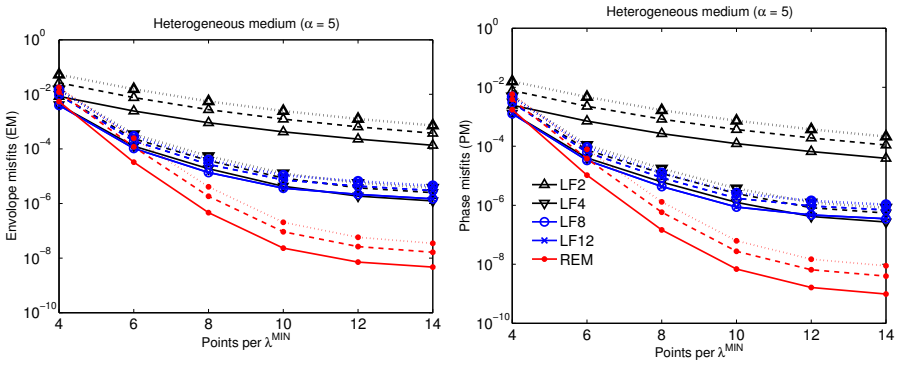

Figure 3: EM and PM errors of LF and REM simulations on a heterogeneous medium ($\alpha = 5$).

Conclusions

On LF simulations of 1D acoustic wave propagation, with an optional medium heterogeneity, fourth- and higher-order time discretizations allow modeling amplitudes and phases with more accuracy than the second-order scheme. For a similar computing cost, the error tolerance reached by the LF4 scheme on grids with 6 *ppw* is almost matched by the LF2 method on meshes twice denser, and then double memory requirements of the latter. Under same time sampling, higher-order LF8 and LF12 schemes behave more precisely than LF4 on a medium with none, or only mild heterogeneities, but their additional computational cost make these methods less attractive. REM integrations based on Chebyshev matrix expansions show a much faster convergence than any of these LF methods on grids with 10 *ppw* and less under same SG spatial discretization (limited to eigth order), and proves that global accuracy can be further improved. However, LF4 seems as the more accurate and equally costly substitute of LF2 on 2-D and 3-D FD SG applications.

References

Blanch, J.O. and Robertsson, J.O.A. [1997] A modified Lax-Wendroff correction for wave propagation in media described by Zener elements. *Geophysical Journal International*, **131**(2), 381–386.

Pestana, R.C. and Stoffa, P.L. [2010] Time evolution of the wave equation using rapid expansion method. *Geophysics*, **75**(4), T121–T131.

Rojas, O., Dunham, E., Day, S.M., Dalguer, L.A. and Castillo, J.E. [2009] Finite difference modeling of rupture propagation with strong velocity-weakening friction. *Geophysical Journal International*, **179**, 1831–1858.

Tal-ezer, H., Kosloff, D. and Koren, Z. [1987] An accurate scheme for seismic forward modelling. *Geophysical Prospecting*, **35**(5), 479–490.